Port-Said Engineering Research Journal

Faculty of Engineering - Port Said University

Volume 23 No. 2 September 2019 pp: 62:71

Analysis of Integrated Cylinder-Shaped Steel Flywheels in Flywheel Energy Storing Systems

Mohammed Saber[1]

Abstract

In this paper, integrated cylinder-shaped flywheels for energy storing are analysed. Two models of integrated flywheels are considered: the "shaftless" flywheel model and the "fully-integrated" flywheel model. In the former model, no shaft is needed; just an axle around which it rotates, and in the later, the flywheel rim is integrated with a hub and a shaft. The models are subjected to a rotational speed of 10,000 rpm. Firstly, theoretical analyses were carried out to derive the equations of the hoop and radial stresses in cylinder-shaped flywheels. In addition, relationships were derived and used, to determine the shape factor K of cylinder-shaped flywheels. The commercial Finite Elements package (Abaqus) was used to model flywheel energy storing systems using axisymmetric elements. It was found that both the shape factor and the energy density (energy stored per kg) of the "shaftless" flywheel are higher than that of the "fully-integrated" flywheel. However, the stress-affected zone in the "fully-integrated" flywheel is less than that in the "shaftless" flywheel. Moreover, it was found that in both models of the flywheel, the maximum generated hoop stress does not depend on the flywheel length, but greatly depends on the rotating speed of the flywheel. In addition, it was concluded that, a thin flywheel has more energy density rather than a thick flywheel if both have the same mass. Both models of the flywheel studied here are suitable to be used in fully-integrated flywheel energy storing systems (FESS). However, the "fully-integrated" flywheel is preferred for its simplicity of assemblage and bearing fixation.

1 Introduction

Flywheel Energy Storing Systems (FESS) are widely used to substitute power interruptions in power supply and to ensure smooth flow of electrical current [1]. The working principal of the FESS is to store kinetic energy into rotating flywheels, and when there is a need of power, this kinetic energy is transferred back to electrical energy flow to the grid. A motor/generator unit (referred to as M/G in the text) is responsible for transferring the electrical energy, from the grid, to rotational kinetic energy in the flywheel (motor mode), and then to transfer the flywheel kinetic energy to electrical energy (generator mode) which is supplied to the grid [1]. Integrating the flywheel with the motor/generator unit could have three different configurations: i) "non-integrated", ii) "partially -integrated" and iii) "fully-integrated" configurations as shown in Error! Reference source not found. [2].

This paper analyses the stresses developed in two designs of the fully integrated flywheels. The first design is called "shaftless" flywheel and the second design is called "fully-integrated" cylinder-shaped flywheel. In the "shaftless" flywheel, there is no need for a shaft; just a fixed axle is needed. In the proposed "fully-integrated" flywheels, the shaft, the hub and the rim of the flywheel are assumed to be manufactured as one part. This can be done by either forging or casting. Forged flywheels provide high strength and therefore can operate at high speeds. In both designs, the motor/generator unit and the bearings are all incorporated in the flywheel cavity. Both models of the flywheel are considered to be made of steel, in this study. The rim of both flywheel models has the same dimensions. However, the total mass of the "fully-integrated" flywheel would be higher than that of the "shaftless" flywheel due to presence of the shaft and the hub. This would results in less energy density of the "fully-integrated" flywheels when compared to "shaftless" flywheels. The "shaftless" flywheel model and the "fully-integrated" flywheel model are, schematically, shown in Figure 2.

Finite Element (FE) method has been widely used to assess the performance of flywheels. For example, Arslan, M. conducted FE studies, using an FE commercial package Ansys, to assess the effects of flywheel geometry on energy density and specific energy (kinetic energy stored by unit volume). He concluded that the energy density of annular discs (can be approximated as short hollow cylinder) is about 70% of that of solid flywheels.[3]. In this study, FE analyses were carried out on long cylinder-shaped flywheels.

Flywheels are classified as either low-speed flywheels or high-speed flywheels. Low-speed flywheels are made of steel and operate at speed up to 30,000 rpm. High-speed flywheels are made of composite materials and operate at speed up to 100,000 rpm [4]. It is hard to manufacture a flywheel-shaft-hub integrated flywheel using composite materials. Therefore, in this study, steel flywheels are considered.

The shape of a flywheel affects its energy density. A shape factor ranges from 0.3 to 1.0, for disc flywheels, address the efficiency of the use of the flywheel material. For the current study, thin rim cylinder-shaped flywheels are used. Thin rim cylinder-shaped flywheels benefit

[1]*Department of Production Engineering and Mechanical Design, Faculty of Engineering, Port Said University, Port Said, Egypt*
email: mssaber77@yahoo.com
Department of Mechanical Engineering, Faculty of Engineering, King Faisal University, Kingdom of Saudi Arabia
email: msaber@kfu.edu.sa
https://dx.doi.org/10.21608/pserj.2019.14198.1004

from the high shape factor they have when compared to disc-shaped flywheel if both have the same mass [5].

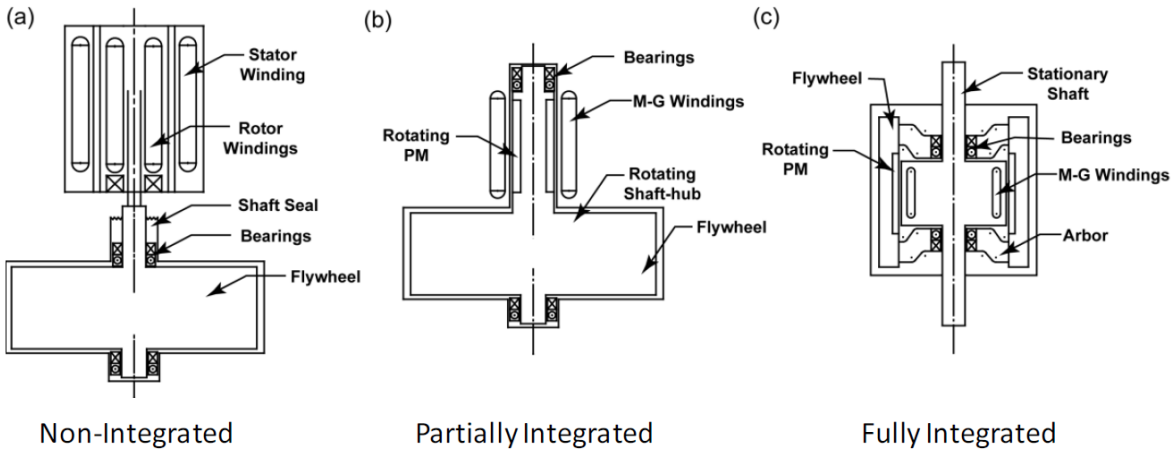

Figure 1: Layout configurations for Flywheel Energy Storing System [2]

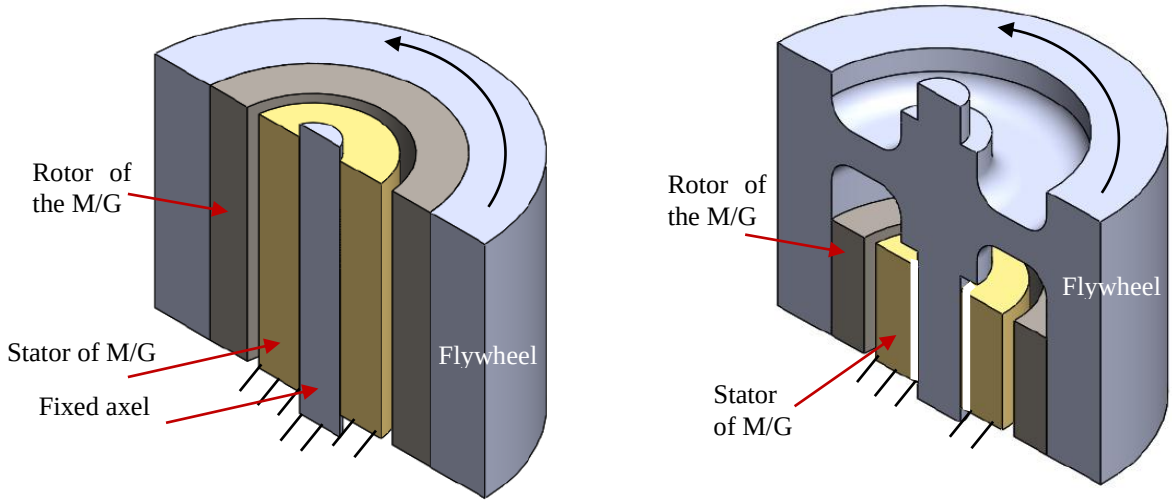

(a) "shaftless" Flywheel

(b) "fully-integrated" flywheel

Figure 2: Simplified sectional view of integrated FESS.

2 Flywheel Stress Analysis

2.1 Disc-shaped flywheel

Flywheels are always designed and manufactured as disc-shaped flywheels. For the disc-shaped flywheel, the equilibrium and compatibility equations are derived as follows for a rotating element of the disc flywheel as shown in Figure 3, with unit thickness.

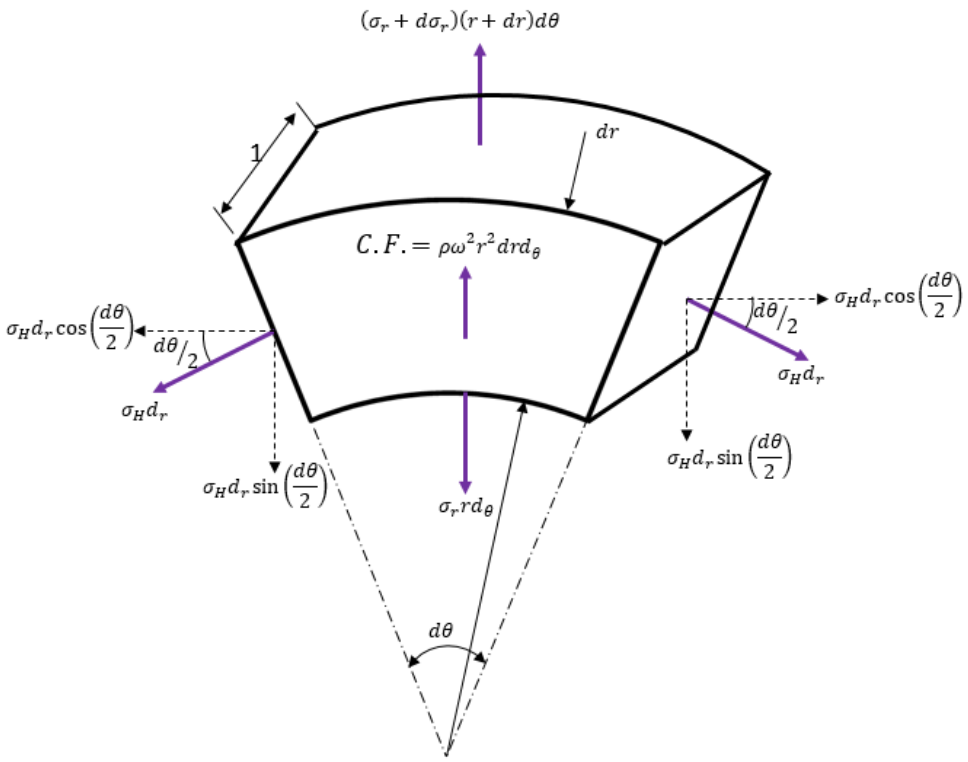

Figure 3: Forces acting on a general element in a rotating disc [6]**. (C.F. = Centrifugal Force)**

The equilibrium of the forces acting in the radial direction indicates that [6];

$$\sigma_r r d_\theta + 2\sigma_H d_r \sin\left(\frac{d_\theta}{2}\right) - (\sigma_r + d\sigma_r)(r+dr)d_\theta = \rho\omega^2 r^2 dr d_\theta \quad \textbf{(1)}$$

where

σ_r	is the radial stress, Pa
σ_H	is the hoop stress, Pa
ρ	density of the flywheel material, kg/m^3
ω	angular speed of the flywheel, rad/s. $\omega = \frac{2\pi n}{60}$ and n in rpm
r	radius of the flywheel, m

The right hand side of equation (1) is the centrifugal force acting on the element. It can be clearly seen that the centrifugal force is a function of the density of the disc material, the disc geometry and its rotating velocity.

By simplifying the brackets in equation (1) and ignoring the high order terms, equation (1) can be further simplified to;

$$\sigma_H - \sigma_r + r\frac{d\sigma_r}{d_r} = \rho\omega^2 r^2 \quad \textbf{(2)}$$

In order to determine the values of σ_H andσ_r, the compatibility equation is needed. As the hoop strain equals to the circumferential strain, the compatibility equation is given by;

$$(\sigma_H - \sigma_r)(1+v) + r\frac{d\sigma_H}{dr} - vr\frac{d\sigma_r}{dr} = 0 \quad \textbf{(3)}$$

where ν is the Poisson's ratio

By substituting equation (3) into equation (2) and integrating with respect to r, the hoop and radial stresses for a solid rotating disc are given by;

$$\sigma_H = \frac{\rho\omega^2}{8}[(3+v)R_o^2 - (1+3v)r^2] \quad \textbf{(4)}$$

$$\sigma_r = \frac{\rho\omega^2}{8}(3+v)[R^2 - r^2] \quad \textbf{(5)}$$

where R_o is the outer radius of the flywheel.

When the disc is perforated with a hole of radius R_i, the radial and hoop stresses are modified to accommodate zero radial stress at the inner surface of the hole. The hoop and radial stresses for a disc with center hole are given by [6]and [7];

$$\sigma_H = \frac{\rho\omega^2}{8}\left[(3+v)\left(R_i^2 + R_o^2 + \frac{R_i^2 R_o^2}{r^2}\right) - (1+3v)r^2\right] \quad \textbf{(6)}$$

$$\sigma_r = \frac{\rho\omega^2}{8}(3+v)\left[R_i^2 + R_o^2 - \frac{R_i^2 R_o^2}{r^2} - r^2\right] \quad \textbf{(7)}$$

where R_i is the inner radius of the disc and R_o is the outer radius of the disc. These equations are applicable under certain restrictions, which are [7]:

- $R_o \geq 20t$ where t is the thickness of the disc.
- The thickness t of the disc is constant.

- Radial and hoop stresses are constant through the thickness

The maximum value of the hoop stress takes place at the inner surface of the disc where r=R_i. It is given by,

$$\sigma_{H\,Max} = \frac{\rho\omega^2}{4}[R_i^2(1-v) + R_o^2(3+v)] \quad \textbf{(8)}$$

From this equation, the maximum angular velocity of the disc-shaped flywheel is given by;

$$\omega_{Max} = \left[\frac{4S_{ut}}{\rho(R_i^2(1-v) + (3+v)R_o^2)}\right]^{1/2} \quad \textbf{(9)}$$

where, S_{ut} is the ultimate tensile strength of the flywheel material.

The kinetic energy at the maximum angular velocity is known as *kinetic energy at burst*$T_{@burst}$, which is given as;

$$T_{@burst} = {}^1\!/_2\left[\frac{m}{2}(R_o^2 + R_i^2)\right]\left[\frac{4S_{ut}}{\rho\left(R_i^2(1-v) + (3+v)R_o^2\right)}\right]$$

which can be simplified to

$$T_{@burst} = \frac{mS_{ut}(R_o^2 + R_i^2)}{\rho(R_i^2(1-v) + (3+v)R_o^2)}$$

and further to

$$T_{@burst} = \frac{mS_{ut}(1+R^2)}{\rho\big((1-v)R^2 + (3+v)\big)} \quad \textbf{(10)}$$

where m is the flywheel mass and R is known as radii ratio, $R = \frac{R_i}{R_o}$

The maximum energy density, e_{max}, is the kinetic energy at burst per unit mass. It can be derived as;

$$e_{Max} = \frac{T_{@burst}}{m} = \frac{1}{m}\frac{mS_{ut}(1+R^2)}{\rho\big((1-v)R^2 + (3+v)\big)}$$

$$e_{Max} = \frac{S_{ut}}{\rho}\frac{(1+R^2)}{(1-v)R^2+(3+v)} = \frac{S_{ut}}{\rho}\,K \quad \textbf{(11)}$$

where, K is defined as shape factor which equals to

$$K = \frac{(1+R^2)}{(1-v)R^2 + (3+v)} \quad \textbf{(12)}$$

2.2 Cylinder-shaped flywheel

Flywheels used in FESS are usually made as either solid discs or hollow cylinders. Cylinder-shaped flywheels are used in order to minimize the volume of the FESS unit and to attain high energy density. In this research, hollow cylinders with inner radius R_i and outer radius R_o are used. The hollow cylinder flywheel is selected to accommodate the rotor of the motor/generator (M/G) unit. Hoop and radial stresses induced in a cylinder-shaped flywheel are given as;

$$\sigma_H = \frac{\rho\omega^2}{8}\left(\frac{3-2v}{1-v}\right)\left[R_i^2 + R_o^2 + \frac{R_i^2R_o^2}{r^2} - \frac{(1+2v)}{(3-2v)}r^2\right] \quad \textbf{(13)}$$

$$\sigma_r = \frac{\rho\omega^2}{8}\left(\frac{3-2v}{1-v}\right)\left[R_i^2 + R_o^2 - \frac{R_i^2R_o^2}{r^2} - r^2\right] \quad \textbf{(14)}$$

The maximum value of the hoop stress takes place at the inner surface of the cylinder where r=R_i. It is given by;

$$\sigma_{H\,Max} = \frac{\rho\omega^2}{8}\left(\frac{3-2v}{1-v}\right)\left[2R_o^2 + 2R_i^2\left(\frac{1-2v}{3-2v}\right)\right]$$

$$\sigma_{H\,Max} = \frac{\rho\omega^2}{4}\left(\frac{3-2v}{1-v}\right)\left[R_o^2 + \left(\frac{1-2v}{3-2v}\right)R_i^2\right] \quad \textbf{(15)}$$

The maximum hoop stress is a life-limiting factor of the flywheel. Its maximum value is the ultimate tensile strength of the flywheel material. Therefore, the maximum attainable angular velocity as a function of the ultimate tensile strength of the flywheel material is;

$$\omega_{Max} = \left[\frac{4S_{ut}(1-v)}{\rho\left((3-2v)R_o^2 + (1-2v)R_i^2\right)}\right]^{1/2} \quad \textbf{(16)}$$

The safe operating angular velocity is determined by applying a factor of safety of 3 to 5 such that [8];

$$Factor\ of\ safety = \frac{\omega}{\omega_{Max}} \cong 3 \to 5$$

2.3 Energy density of cylinder-shaped flywheel

The kinetic energy, T, of a flywheel is given by;

$$T = \frac{1}{2}I\omega^2 \quad \textbf{(17)}$$

where, I is the mass moment of inertia of the wheel and ω is the flywheel's angular velocity. For a hollow cylinder with mass m, inner radius R_i and outer radius R_o, I is given by;

$$I = \frac{m}{2}(R_o^2 + R_i^2) \quad \textbf{(18)}$$

Equations (17) and (18) indicate that when the mass of the flywheel is doubled, the kinetic energy is doubled, too. However, when the angular velocity is doubled, the kinetic energy is quadrupled. General speaking, the faster a flywheel rotates the more energy it stores.

The kinetic energy for a cylinder-shaped flywheel at burst speed is simply obtained by substituting the value of ω_{Max}, from equation (16) and I, from equation (18), in equation (17) as;

$$T_{@burst} = {}^1\!/_2\left[\frac{m}{2}(R_o^2 + R_i^2)\right]\left[\frac{4S_{ut}(1-v)}{\rho\left((3-2v)R_o^2 + (1-2v)R_i^2\right)}\right]$$

$$T_{@burst} = \frac{m\,S_{ut}(1-v)(R_o^2+R_i^2)}{\rho\left((3-2v)R_o^2+(1-2v)R_i^2\right)} \quad \textbf{(19)}$$

The energy density of the flywheel is defined as;

$$e = \frac{T}{m} \quad \textbf{(20)}$$

Substituting equation (19) into equation (20), the maximum attainable energy density is then given as:

$$e_{Max} = \frac{m\,S_y(1-v)(R_o^2+R_i^2)}{m\rho\left((3-2v)R_o^2+(1-2v)R_i^2\right)}$$

$$= \frac{S_{ut}}{\rho}\frac{(1-v)(R_o^2+R_i^2)}{(3-2v)R_o^2+(1-2v)R_i^2} = \frac{S_{ut}}{\rho}K \quad \textbf{(21)}$$

where, K is defined as shape factor and is given, for the cylinder shape flywheel, as:

$$K = \frac{(1-v)(1+R^2)}{(1-2v)R^2+3-2v} \quad \textbf{(22)}$$

It is worth mentioning that equation (22) defines the shape factor for a cylinder-shaped flywheel when no material or geometry nonlinearities are present and only hoop stress was considered.

2.4 Shape factor, K

For flywheels having the same mass, their energy density could differ based on the shape of each flywheel. The effect of the shape of the flywheel is characterized by a shape factor K. The shape factor K depends mainly on the polar moment inertia of the flywheel, I. The value of K for flywheel designs ranges from 0.3 to 1.0, where K = 1.0 is a theoretical case, which is taken as a reference to which other designs are related. Specific energy and energy density is related to the shape factor by (e.g. [9] and [10]);

$$e_V = \frac{T}{V} = KS_{ut}$$
$$e_m = \frac{T}{m} = K\frac{S_{ut}}{\rho}$$

where e_v, e_m and V are the specific energy, the energy density and the flywheel volume, respectively.

For K=1, i.e. the hypothetical maximum attainable shape factor, the energy density is given as:

$$e_m = \frac{\frac{1}{2}I\omega^2}{m} = \frac{S_{ut}}{\rho}$$

from which, the maximum angular velocity is obtained as:

$$\omega_{@K=1} = \sqrt{\frac{2mS_{ut}}{\rho I}}$$

Substitute this value of angular speed into equation (15) to get the maximum theoretical hoop stress that material can withstand as follow;

$$\sigma_{H\omega@K=1} = \frac{\rho\omega_{@K=1}^2}{4}\left(\frac{3-2v}{1-v}\right)\left[R_o^2+\left(\frac{1-2v}{3-2v}\right)R_i^2\right]$$

$$\sigma_{H\omega@K=1} = \frac{m}{2}\frac{S_{ut}}{I}\left(\frac{3-2v}{1-v}\right)\left[R_o^2+\left(\frac{1-2v}{3-2v}\right)R_i^2\right] \quad \textbf{(23)}$$

In fact, this value of the hoop stress is greater than the actual value of stress the flywheel material can withstand. The ratio between this theoretical value and actual value equals to the actual shape factor of the flywheel. This means, the actual value of the shape factor K can be obtained as:

$$K = \frac{S_{ut}}{\sigma_{H\omega@K=1}} \quad \textbf{(24)}$$

The actual maximum operating angular speed, ω_{max}, can be obtained using:

$$\omega_{max} = \sqrt{K}\omega_{@K=1}$$

3 Finite Element Modelling

The finite element commercial package, Abaqus, was used to analyze the "shaftless" and the "fully-integrated" flywheels. Firstly, a "shaftless" flywheel was modelled to conduct mesh study and to study the effects of the rim length on the generated hoop stress. Secondly, an FE model of "fully-integrated" flywheel was created to determine the position and the value of the maximum stresses acting on it. For both of the models, four nodes axisymmetric reduced integration elements, designated as CAX4R in Abaqus [11], were used. The modelling parameters are given in Table 1.

Table 1: FE modelling parameters

flywheel material	Steel
modulus of Elasticity, E (GPa)	210
Poisson's ratio, ν	0.3
rotational velocity (rpm)	10,000

Figure 4 (a) shows the axisymmetric FE model of the "shaftless" flywheel while Figure 4 (b) shows a 180° revolved view of the model. This is shown for the sake of clarity of the flywheel hollow cylindrical nature. The FE model of the "fully-integrated" flywheel is shown in Figure 5. It worth noting that, only the mechanical components, i.e. the rim, the hub and the shaft, of the flywheel are shown in the model. Electrical parts, i.e. permanent magnets, the Motor/Generator unit, are removed to simplify the modelling process and they have no effects of the generated stresses.

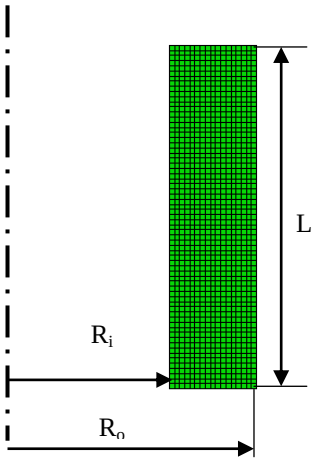

(a) the axisymmetric model

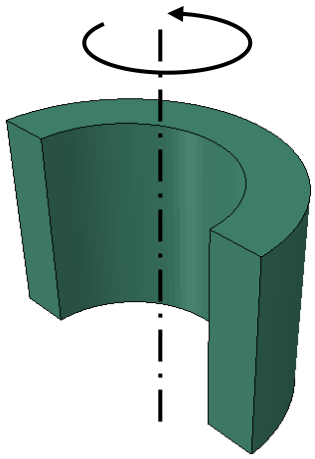

(b) a 180° revolved view of the "shaftless" flywheel model

R_i = Inner radius, R_o= Outer radius and L=Rim length

Figure 4: FE model of the "shaftless" flywheel.

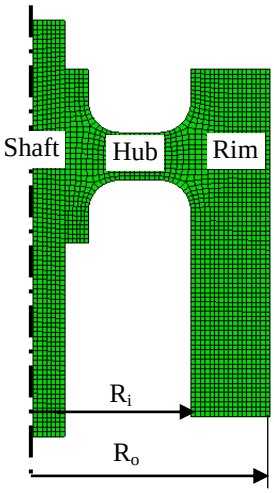

(a) the axisymmetric model

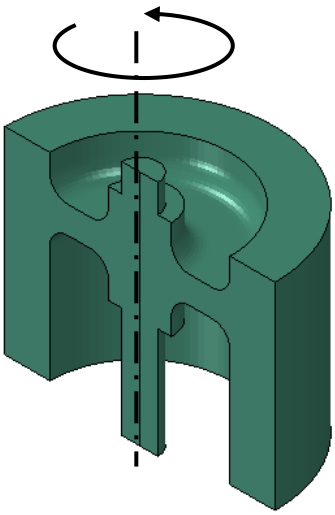

(b) a 180° revolved view of the "fully-integrated" flywheel model

R_i = Inner radius and R_o= Outer radius

Figure 5: FE model of the "fully-integrated" flywheel.

4 Results and Discussion

4.1 Mesh Study

Mesh study was carried out to check the results sensitivity to the element size. Meshes with element size ranges from 0.25 mm, extremely fine mesh, to 25 mm, extremely coarse mesh, were used. The "shaftless" model was used with rotating speed of 10,000 rpm. Figure 6 shows the maximum obtained hoop stress for different element sizes compared to the theoretically calculated results. It can be seen that the finer the element size the more accurate results obtained. It is worth noting that the minimum and the maximum errors between the FE calculated hoop stress and the theoretically calculated hoop stress are 2% and 14%, respectively. Element size of 3 mm were used in this study.

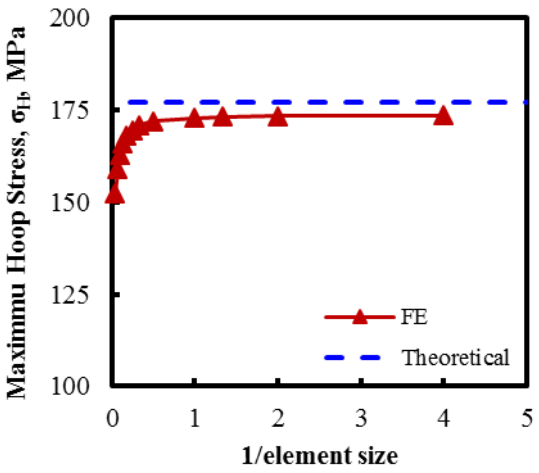

Figure 6: Mesh study of the FE used models.

4.2 Stresses in cylinder-shaped flywheels

Three stresses are developed in the rotating flywheel: the hoop stress, the radial stress and the axial stress. Figure 7 plots the distribution of the hoop stress for a cylinder-shaped flywheel obtained using equation (13) at different rotating speeds. The distribution of the radial stress at 10,000 rpm is also shown. It can be seen that, the hoop stress is always tensile stress with its maximum value is at the inner surface of the flywheel. In addition, the radial stress is zero at the inner and outer surfaces of the flywheel as these surfaces are free to expand surfaces. It can, also, be seen that, at 10,000 rpm, the hoop stress is about 25 times that of the radial stress. This emphasizes the severity of the hoop stress in the rotating flywheel as a life-limiting factor. In addition, it is notable that as the rotating speed increases the difference in the hoop between the inner and the outer surfaces increases. The maximum value of the hoop stress is changing non-linearly with the flywheel rotating speed, see Figure 8.

4.3 Determination of burst rotational speed

The burst rotational speed for a flywheel is a function of its material strength and the flywheel dimensions see equation (16). For the current study, by substituting the values of R_i=100 mm, R_o=150 mm, ν=0.3 and ρ=7800 kg/m^3 into equation (16), the maximum allowable angular velocity equals to 1760 rad/s which is equivalent to 16800 rpm. It is worth noting that, this value of the rotational speed is independent of the rim length, as it will be shown in Section 4.5. In the current study, the flywheel is assumed to run at 10,000 rpm, which is 60% of the burst speed.

FE analyses were used to determine the burst rotating speed for both the "shaftless" and the "fully-integrated" flywheels, see Figure 8. For the "shaftless" flywheel, the FE obtained results were compared to theoretical results obtained using equation (16). It can be seen that the FE results and the theoretical results are identical. The burst stress obtained using equation (16) is also shown in Figure 8. The area bounded by the dash line is the safe operating area where the maximum generated hoop stress is always less than the material tensile stress.

4.4 Shape factor and energy density

The shape factor K defines how efficient the flywheel material is used to store energy. The shape factor for a constant thickness isotropic cylinder-shaped flywheel can be calculated from equation (22). Figure 9 shows the relationship between the shape factor K and the energy density e, and the radii ratio R. The flywheel material is steel with the density of 7800 Kg/m^3, tensile strength of 500 MPa and Poisson ratio of 0.3. It can be seen that when R approaches zero, i.e. solid disc flywheel, K=0.3 and when R approaches one, i.e. very thin rim flywheel, K=0.5. Moreover, Figure 9 shows that for the ratio of R less than 0.2, the shape factor is almost constant around 0.3. For R>0.2, the value of the shape factor increases as R increases. In other words, as the flywheel rim gets thinner, its shape factor gets higher. It can be concluded that, for constant values of tensile strength, S_{ut}, and the material density, ρ, it can be seen that the shape factor and, hence, the energy density increases with increasing the value of radii ratio R. In industry, the value of R ranges from 0.5 to 0.75. These values enable the designers to allocate the M/G unit inside the flywheel easily[8].

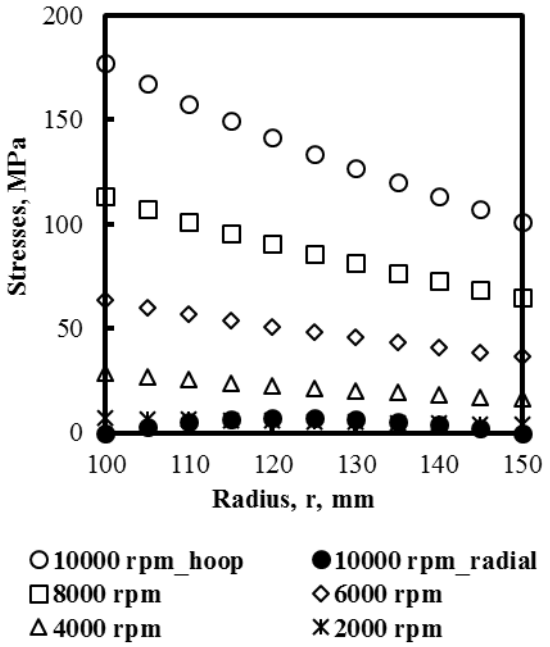

Figure 7: Hoop and radial stresses for cylinder-shaped flywheel at different rotational speed. R_i=100mm and R_o=150mm.

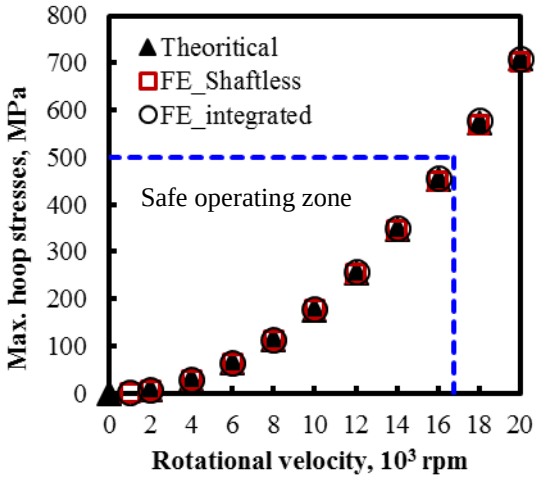

Figure 8: Maximum hoop stress against rotational velocity of cylinder-shaped flywheel.

Alternatively, Figure 10 shows the relationship between the energy density, e, the shape factor, K, and the 1/R ratio (i.e R_o/R_i). It can be seen that the energy density and the shape factor are constant for very thick flywheels where $R_o/R_i > 5.0$. This indicate that it might be a waste of material to use very thick flywheels. Alternatively, multiple thin flywheels are recommended in order to store higher kinetic energy.

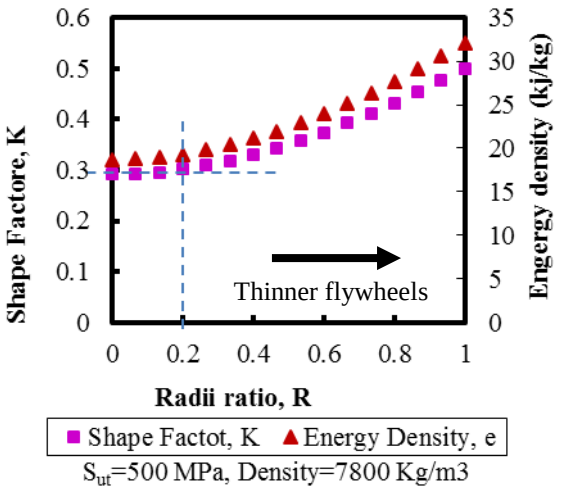

Figure 9: Relationship between maximum energy density, e_{max}, shape factor, K, and radii ratio, R.

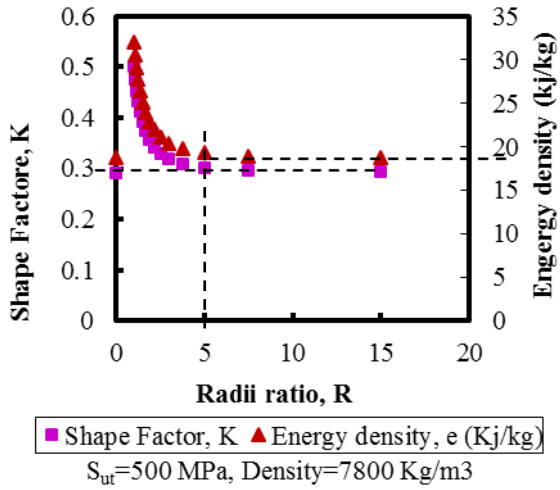

Figure 10: Relationship between energy Density, e, shape factor, K, and Radii ratio.

For the flywheel models used in this study, Table 2 contains the geometrical and mass properties obtained using the Solidworks software [12]. The data given were used to calculate the energy density of each model. It can be seen that energy density of the "shaftless" model is higher than that for the "fully-integrated" model. This is because the mass of the "fully-integrated" model is higher due to the mass of the shaft and the hub.

Table 2: Energy density and shape factor for "shaftless" and "fully-integrated" flywheel models.

	"shaftless" model	"fully-integrated" model
Mass (kg)	61.26	79.79
polar mass moment of inertia, I, (kg/m^2)	1	1.14
radii ratio, R	0.67	0.67
rotating speed (rpm)	16,800	16,800
angular velocity (rad/s)	1759	1759
max. stored Energy (kj)*	1540	1766
energy density (kj/kg)	25	22
shape factor, K**	0.39	0.39
shape factor, K***		
* calculated using equation (19) ** determined from Figure 9 *** determined using equation (24)		

4.5 Effect of flywheel length

Flywheels are usually made as thin discs with the shape selected in such a way that its shape factor is maximum. However, for the cylinder-shaped flywheels, the length of the flywheel should be considered. FE analyses were carried out using the "shaftless" axisymmetric model, shown in Figure 11. The model material is selected as steel with E=210 GPa and Poisson's ratio, ν, of 0.3 and density of 7800 kg/m^3. The flywheel was modelled as a hollow cylinder with inner diameter 100 mm and outer diameter of 150. Five models were used with length range from 40 mm to 200 mm in step of 40 mm. All the models were rotated at

10,000 rpm. The values of the maximum hoop stress for each model is plotted against the flywheel length as shown in Figure 12. It can be clearly seen that the maximum hoop stress is independent of the flywheel length. In addition, the FE results agree well with the theoretical results calculated using equation (13).

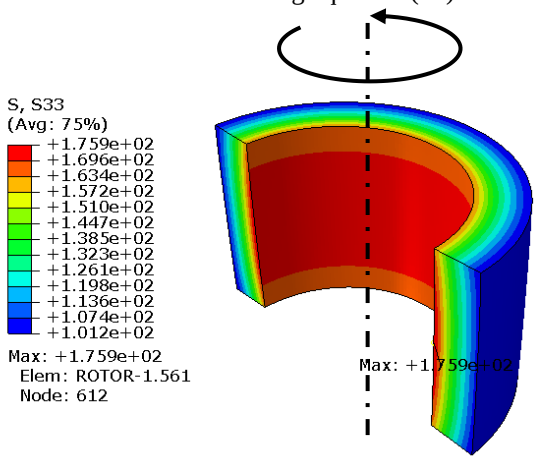

Figure 11: Sectional view of the "shaftless" flywheel. The maximum hoop stress acts at the inner surface of the flywheel. Stress is in MPa.

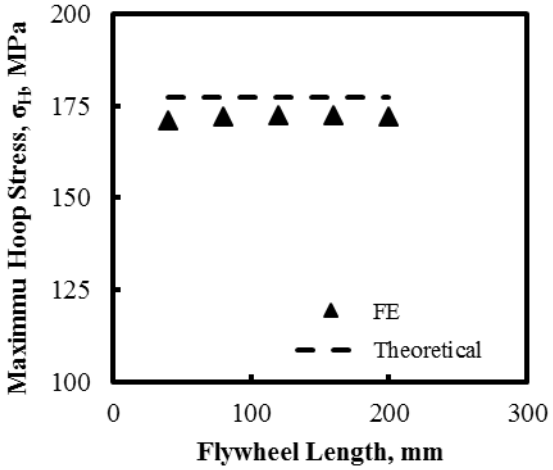

Figure 12: Maximum hoop stress acting on the cylinder-shaped flywheel is length independent.

4.6 Stresses in "fully-integrated" flywheel.

Figure 13 shows the hoop stress developed in the "fully-integrated" flywheel when it rotates at 10,000 rpm. It can be seen that, similar to the "shaftless" flywheel, the maximum hoop stress takes place at the inner surface of the flywheel but at smaller area. The support provided to the flywheel by the hub and the shaft reduces the hoop stress values in most of the inner surface of the flywheel. It can be deduced that if the hub is placed at the middle of the flywheel, the stress affected zone would be smaller than the current situation. As mentioned, positing the hub at the top of the flywheel is desired to accommodate the motor/generator unit inside the flywheel. In addition, it can be seen that stresses acting on the shaft is significantly small. This is because the hoop stress is greatly dependent on the radius of the rotating parts.

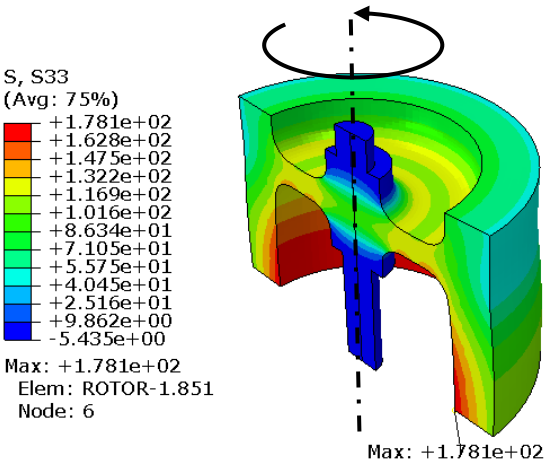

Figure 13: Sectional view of the "fully-integrated" flywheel. The maximum hoop stress acts at the inner surface of the flywheel values of stress is in MPa

5 Conclusion

Flywheels are used as energy storing devices in energy storing systems. It has several advantages over other energy storing system, such as batteries. However, stresses generated in it are life-limiting factors. In this paper, fully-integrated flywheels are analyzed. The fully-integrated" flywheels could be "shaftless" flywheels or flywheels which are "fully-integrated" with a shaft and a hub. Theoretical analysis was firstly carried out and then FE analyses were run for the "shaftless" and the "fully-integrated" flywheels.

The value of the shape factor K indicates how efficient the flywheel material was used to store energy. The value of K depends on the flywheel dimensions and material. It was found that, the shape factor K for cylinder-shaped flywheel with radii ratio R of 0.2 or less is almost the same, about 0.3. For R>0.2, the shape factor K increases with R until it hits its maximum value of 0.5 when R equals to one. The increase of the shape factor means an increase in the energy that can be stored in the flywheel. These results show that, in terms of stored energy, thin long flywheels are better than short thick flywheels providing that the both flywheels have the same mass. For non-standard flywheels, such as the "fully-integrated" flywheel in this study, it is suggested to use equation (24) to find the value of K.

It was concluded that the maximum hoop stress developed in flywheels is independent of the flywheel length. In addition, it was found that both theoretical analyses and the FE analyses could predict the maximum value of the rotational speed a flywheel can run at.

6 References:

[1] Amiryar,M. E. and Pullen,K. R., "A review of flywheel energy storage system technologies and their applications," Applied Sciences, (2017), vol. 7, no. 3.

[2] Hearn,C. S., “Design methodologies for advanced flywheel energy storage,” The University of Texas at Austin, 2013.
[3] Arslan,M. A., “Flywheel geometry design for improved energy storage using finite element analysis,” Materials and Design, (2008), vol. 29, pp. 514–518.
[4] Gyuk,I. P., “EPRI-doe handbook of energy storage for transmission and distribution applications,” Washington,.
[5] Östergård,R. and Östergård,R., “Flywheel energy storage a conceptual study flywheel energy storage - a conceptual study,” Uppsala Universitet, 2011.
[6] Hearn,E. J., “Mechanics of Materials,” 3rd ed. Oxford: Butterworth-Heinemann, 2000.
[7] Budynas,R. G. and Nisbett,J. K., “Shigley’s Mechanical Engineering Design,” 10th ed. New York: McGraw-Hill Education, 2015.
[8] Lovejoy,A. E. and Poplawski,S., “Preliminary design and analysis of an in-plane prseus joint,” 54th AIAA/ASME/ASCE/AHS/ASC Structures, Structural Dynamics, and Materials Conference, (2013), no. May.
[9] Bankston,S. and Mo,C., “Geometry modification of flywheels and its effect on energy storage,” Energy Research Journal, (2015), vol. 6, no. 2, pp. 54–63.
[10] Conteh,M. A. and Nsofor,E. C., “Composite flywheel material design for high-speed energy storage,” (2016), vol. 14, pp. 184–190.
[11] Dassault Systemes, “Abaqus.” 2015.
[12] Dassault Systèmes, “Solidworks.” 2016.